Chemistry–A European Journal
Research Article
doi.org/10.1002/chem.202104535
Chemistry Europe
European Chemical Societies Publishing
www.chemeurj.org

# Luminescent Pyrrole-Based Phosphaphenalene Gold Complexes: Versatile Anticancer Tools with Wide Applicability

Valentina Fermi[+],[a] Elzbieta Regulska[+],[b, c] Anna Wolfram[+],[b, c] Patrick Wessling,[c] Frank Rominger,[c] Christel Herold-Mende,*[a] and Carlos Romero-Nieto*[b, c]

**Abstract:** Brain cancer, one of the most lethal diseases, urgently requires the discovery of novel theranostic agents. In this context, molecules based on six-membered phosphorus heterocycles – phosphaphenalenes – are especially attractive; they possess unique characteristics that allow precise chemical engineering. Herein, we demonstrate that subtle structural modifications of the phosphaphenalene-based gold(I) complexes lead to modify their electronic distribution, endow them with marked photophysical properties and enhance their efficacy against cancer. In particular, phosphaphenalene-based gold(I) complexes containing a pyrrole ring show antiproliferative properties in 14 cell lines including glioblastomas, brain metastases, meningiomas, IDH-mutant gliomas and head and neck cancers, reaching $IC_{50}$ values as low as 0.73 μM. The bioactivity of this new family of drugs in combination with their photophysical properties thus offer new research possibilities for both the fundamental investigation and treatment of brain cancer.

## Introduction

Cancer is one of the most severe and deadly diseases of humankind. Despite major efforts in the field of pharmaceutical chemistry, cancer remains the second leading cause of death globally.[1] In particular, brain malignancies are characterized by high morbidity and mortality rates. Due to localization and invasiveness, brain malignancies are commonly associated with resistance to treatment and poor treatment outcome.[2]

Gliomas are the most common primary malignant brain tumors in adults and, among them, glioblastoma multiforme (GBM, WHO °IV) is the most prevalent and aggressive.[3] GBM is considered to be one of the most lethal cancers in adults with only 35% of patients surviving the first year after diagnosis and few patients reaching the long-term survival status of 2.5 years post-diagnosis.[4] The current standard-of-care (SOC) includes maximal-safe surgical resection, radiation and concurrent as well as adjuvant chemotherapy with the alkylating agent temozolomide (TMZ). Despite multimodal treatment regimens, GBM patients have a median survival of 15 months.[5] The problem is that recurrences occur in 90% of all cases around 7 months after resection of the primary tumor;[6] this is mostly because removing 100% of the tumor from the brain without damaging it is not possible. Another problem is that the patient characteristics including genetic and epigenetic changes strongly influence the treatment prognosis. In fact, only 45% of patients will respond to therapies with alkylating agents. The reason is that the *O*-6-methylguanine-DNA methyltransferase (MGMT) DNA-repair gene ultimately revokes the therapeutic effects of alkylating agents like TMZ; its silencing by promoter methylation leads thus to an improved overall, progression-free survival in patients treated with TMZ and radiotherapy.[7,8] However, only 45% of GBM patients exhibit methylated MGMT promoters.[7,9] Thus, the urgent scientific challenge is to develop novel non-alkylating anti-GBM molecules, which could act independently from the MGMT promoter methylation status.

In this context, we recently developed a novel family of anticancer gold(I) complexes based on six-membered phosphorus-containing heterocycles – the phosphaphenalenes (Scheme 1a).[10] The unique architecture of the phosphaphenalenes synergistically merges the advantages of five- and six-membered phosphorus heterocycles (e.g., the versatility at the phosphorous center and the electronic delocalization)[11] and therefore represents a unique gold(I) ligand. As such, the phosphaphenalenes offer outstanding structural and electronic

[a] *Dr. V. Fermi,[+] Prof. Dr. C. Herold-Mende*
*Division of Neurosurgical Research, Department of Neurosurgery*
*Ruprecht-Karls-Universität Heidelberg*
*Im Neuenheimer Feld 400, 69120 Heidelberg (Germany)*
*E-mail: H.Mende@med.uni-heidelberg.de*

[b] *Dr. E. Regulska,[+] A. Wolfram,[+] Prof. Dr. C. Romero-Nieto*
*Faculty of Pharmacy*
*University of Castilla-La Mancha*
*Calle Almansa 14 – Edif. Bioincubadora, 02008 Albacete (Spain)*

[c] *Dr. E. Regulska,[+] A. Wolfram,[+] Dr. P. Wessling, Dr. F. Rominger, Prof. Dr. C. Romero-Nieto*
*Organisch-Chemisches Institut*
*Ruprecht-Karls-Universität Heidelberg*
*Im Neuenheimer Feld 270, 69120 Heidelberg (Germany)*
*E-mail: carlos.romero.nieto@oci.uni-heidelberg.de*

[+] *These authors contributed equally to this work.*

*Supporting information for this article is available on the WWW under https://doi.org/10.1002/chem.202104535*

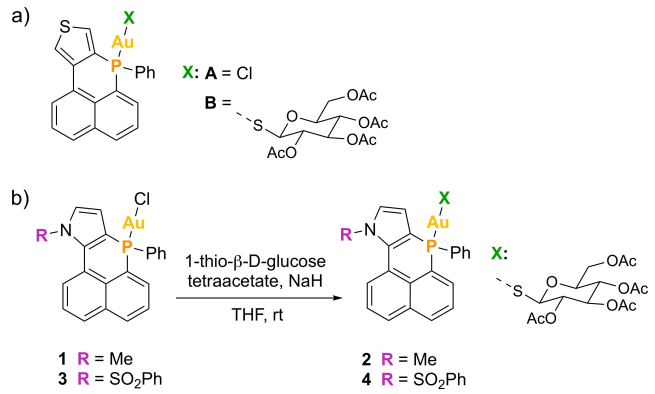


**Scheme 1.** a) First-generation phosphaphenalene-gold(I) drugs **A** and **B**; b) Synthesis of second-generation gold(I) complexes **1**–**4**.

characteristics; their particular balance between positive and negative hyperconjugation at the phosphorus atom leads to a special electronic environment that clearly distinguishes them from the previously known organophosphorus molecules.[12–20] In addition, phosphaphenalenes offer a vast number of selective post-functionalization reactions at the phosphorous as well as the main scaffold.[11,21,22] Thus, various structural analogs can readily be accessed, which is of immense value as it allows to easily finetune the desired chemical characteristics including solubility, stability, lipophilicity and lability; thereby, one can control biorelevant parameters such as bioavailability and cytotoxicity. In fact, we employed a first generation of phosphaphenalene–gold(I) complexes against GBM in pre-clinical studies. The results were remarkable. Replacing the chloride from the gold atom (Compound **A**, Scheme 1) with a thio-sugar derivative (Compound **B**, Scheme 1) decreased the half-maximal inhibitory concentration ($IC_{50}$) values one order of magnitude reaching the low-micromolar range.[10] Note that the lower the $IC_{50}$ values, the more efficient the drug is. Furthermore, the complexes demonstrated antiproliferative potential, sensitized the cancer cells to apoptosis and hampered cell migration for conventional as well as stem cell-like glioblastoma cells.[10]

Encouraged by these findings, we set out to develop improved second-generation phosphaphenalene-gold(I) complexes. In particular, detailed structural analyses of first-generation gold complexes triggered the following scientific questions: a) Do the structural features of the phosphaphenalene ligands significantly impact the bioactivity of the molecules? b) Does the sulfur from the thiophene of the first-generation drugs contribute to the respective bio-performances? c) Could the bio-activity of the phosphaphenalene gold complexes be improved? d) Would it be possible to provide the molecules with additional properties that allow future investigations on the mode of action *in vivo*?

## Results and Discussion

To provide an answer to the latter scientific questions, we herein present an in-depth structural analysis of a second-generation phosphaphenalene-gold(I) complexes and their antitumor activity. In particular, we investigated to what extent the structural features of the phosphaphenalenes impact the respective bioactivity. Here, the contribution to the bio-performance of chemical moieties fused at the phosphaphenalene ligands (such as the thiophene or pyrrole) is evaluated for each drug analog.

First, we began with the investigation of compound **1** (Scheme 1) (see the Supporting Information for experimental details). It presents a pyrrole moiety fused with a phosphaphenalene core, which is coordinated to an AuCl fragment. Pyrrole-containing phosphaphenalenes are stable and have demonstrated outstanding optoelectronic properties in the context of material science; they possess fluorescence quantum yields up to 80% and have been employed in photoelectrochemical cells,[22] organic light-emitting diodes[23,24] and electrofluorochromic devices.[23] Thus, they could potentially provide drugs with significant spectroscopic properties, which are of particular value for mechanistic investigations *in vivo*. The structure of **1** was unequivocally assigned by single-crystal X-ray analysis (Figure 1, Table S1 in the Supporting Information). It exhibits P–Au and Au–Cl bond lengths of 2.2273(17)[21] and 2.2966(11) Å, respectively (Table S2). These bond lengths are

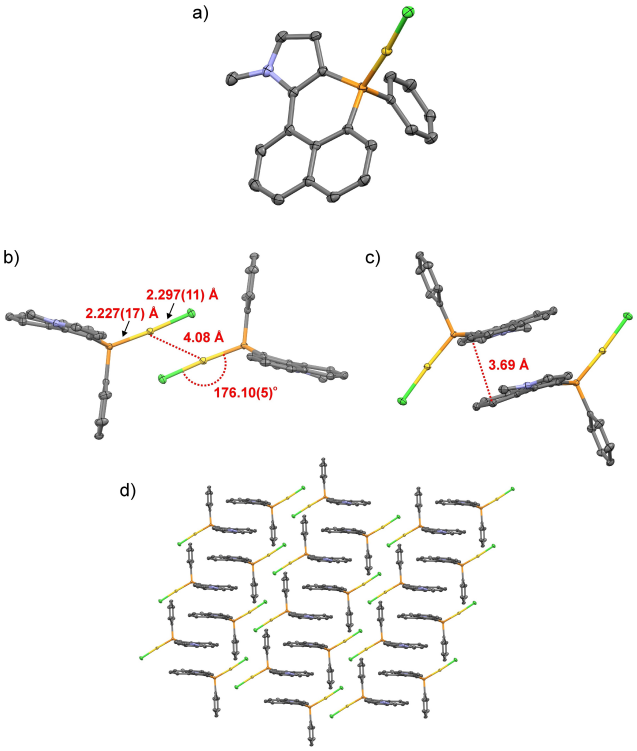


**Figure 1.** X-ray structures of **1** (ellipsoids at 50% probability level). a) Single molecule; b) dimeric structure with P–Au, Au–Cl, Au···Au distances and P–Au–Cl angle, c) dimeric structure with π–π stacking distance, d) crystal packing. Hydrogen atoms have been omitted for clarity.

essentially the same for the analog compound **A** (Table S2). Contrasting physicochemical properties from the P–Au linkage of both compounds were therefore discarded. In the solid state, **1** forms a well-organized 3D pattern (Figure 1). Molecules pile up along one axis leading to columns that interact with each other through Au···Au interactions. This strongly differs from the somewhat more disordered structure of **A**.[21] The Au···Au distances of **1** (4.06 Å) are nevertheless significantly larger than for **A** (3.51 Å). All in all, π–π interactions with intermolecular distances of 3.69 Å in combination with aurophilic interactions appear as driving forces for the packing of **1**.

Compound **1** was furthermore transformed into **2**, an analog compound to **B** (Scheme 1), by replacing the chloride atom with the 3,4,5-triacetyloxy-6-(acetyloxymethyl)oxane-2-thiolate. As described earlier for **B**,[10] compound **2** showed stark reluctance to crystallize; all attempts to obtain its X-ray structure were unsuccessful. To analyze the impact of additional structural modifications on the bioactivity, we replaced the methyl substituent of the pyrrole by a bulkier substituent, that is, the phenylsulfonyl, to afford compound **3** and synthesized the corresponding derivative **4** with a 3,4,5-triacetyloxy-6-(acetyloxymethyl)oxane-2-thiolate moiety (Scheme 1) (see Supporting Information for details). The structural modifications led to changes into the molecules' electronic distribution; these are reflected in the $^{1}$H NMR (Figure 2). Compared with the reference compound **C** (Figure 2), which contains an oxidized, pentavalent phosphorus atom, the biggest $^{1}$H NMR shift in **1** is seen for the protons **a** of the exocyclic ring (Figure 2); they are shielded upon replacing the oxygen at the phosphorus atom by an AuCl moiety. The substitution of the Cl atom of **1** by the sugar derivative 3,4,5-triacetyloxy-6-(acetyloxymethyl)oxane-2-thiolate to yield **2** only induced slight changes (Figure 2). However, the N-substituents had a major impact. Introducing a phenylsulfonyl group at the nitrogen of the pyrrole-fused phosphaphenalene led to a dramatic deshielding of the proton **c** of the pyrrole fragment and proton **b** of the naphthalene (Figure 2).

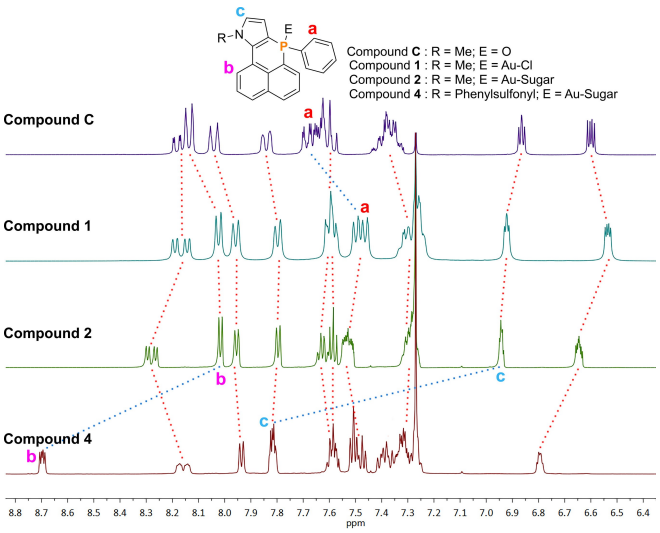


**Figure 2.** $^{1}$H NMR (400 MHz, $CDCl_3$) shifts of compounds **C**, **1**, **2** and **4** upon structural modification.

In turn, while the chloride derivatives **A** and **1** present a singlet at 2.6 ppm in the $^{31}$P NMR (Table S3, Figure S1), **3** displays a signal at 5.6 ppm as a result of the electron-withdrawing effect from the phenylsulfonyl group.[25] On the other hand, all sugar derivatives **B**, **2** and **4** present distinctly deshielded $^{31}$P NMR at 8.2, 9.1 and 9.5 ppm. These values are significantly lower than those observed for previously reported bioactive phosphole- and phosphine-based gold complexes,[26–29] which range between 32–47 ppm.

After analyzing the structural features of the gold derivatives, we turned to *in vitro* experiments. To investigate the impact of the fused phosphaphenalene ring on the bioactivity of the drug, we first focused on the ability of **1** to inhibit cell proliferation in the glioblastoma cell lines NCH82, NCH89 and NCH149. To this end, cells were incubated with increasing concentrations of **1** and cell proliferation was evaluated by crystal violet assay. Compound **1** showed antiproliferative effects in all three cell lines. The mean $IC_{50}$ values for cell lines NCH82, NCH89 and NCH149 were 8.1, 15.1 and 8.87 μM, respectively (Table 1, Figure S2). These values are slightly lower than those found for compound **A**, that is, $IC_{50}$ values of 11.4

**Table 1.** Antiproliferative effects of compounds **A**, **B** and **1**, **2** and **4** upon treatment of cell lines from five types of cancer (expressed as mean of three biological replicates ± standard deviation).

| | Mean $IC_{50}$ value [μM] | | | | |
|---|---|---|---|---|---|
| Cell line | A | B | 1 | 2 | 4 |
| NCH82[a] | 11.4 ± 0.11 | 1.44 ± 0.16 | 8.1 ± 0.62 | 0.73 ± 0.12 | 1.37 ± 0.06 |
| NCH89[a] | 17.3 ± 1.02 | 2.9 ± 0.41 | 15.1 ± 0.66 | 4.00 ± 0.26 | 4.49 ± 0.12 |
| NCH149[a] | – | 3.01 ± 0 | 8.87 ± 0.45 | 0.87 ± 0.12 | 2.85 ± 0.17 |
| NCH517[b] | – | – | – | 1.60 ± 0.30 | – |
| NCH604a[b] | – | – | – | 1.86 ± 0.14 | – |
| NCH466[b] | – | – | – | 1.01 ± 0.02 | – |
| NCH93[c] | – | – | – | 1.35 ± 0.09 | – |
| BenMen-1[c] | – | – | – | 1.32 ± 0.12 | – |
| NCH551b[d] | – | – | – | 1.23 ± 0.25 | – |
| NCH1681[d] | – | – | – | 0.88 ± 0.29 | – |
| NCH3763[d] | – | – | – | 5.21 ± 0.31 | – |
| HNO210[e] | – | – | – | 1.10 ± 0.08 | – |
| HNO199[e] | – | – | – | 2.65 ± 0.25 | – |
| HNO97[e] | – | – | – | 5.51 ± 1.04 | – |

[a] Glioblastoma. [b] Brain metastasis. [c] Meningioma. [d] IDH-mut. glioma. [e] Head and neck cancer.

and 17.3 μM for NCH82 and NCH89, respectively. Thus, modifying the phosphaphenalene core by replacing the thiophene moiety with a pyrrole ring leads to an improved antiproliferative activity *in vitro*.

In line with previous observations,[10] replacing the chloride atom at the gold moiety by a sugar derivative remarkably increased the bioactivity of the drug (Table 1). Compound **2** (Scheme 1) showed mean $IC_{50}$ values one order of magnitude lower than **1**, reaching sub-micromolar concentrations, that is, 0.73, 4.00 and 0.87 μM for cell lines NCH82, NCH89 and NCH149, respectively (Table 1, Figure S3). Again, these values are notably lower than those of the analog compound **B** (Table 1), which contains a phosphaphenalene fused to a thiophene ring (Scheme 1) instead of a pyrrole heterocycle. For comparison, note that the $IC_{50}$ values of Carmustine (an established drug for the treatment of glioblastoma) and the phosphole-based thio-sugar analog of **2** (a more cytotoxic drug than auranofin[30]) with, for example, NCH82 cells are 385[31] and 0.9[27] μM, respectively. In turn, introducing a phenylsulfonyl fragment at the nitrogen of the phosphaphenalene core (compound **4**) led to higher bioactivity compared to **1**. However, values are slightly lower than those of the N-methyl derivative **2**. The mean $IC_{50}$ values for **4** were 1.37, 4.49 and 2.85 μM for glioblastoma cell lines NCH82, NCH89 and NCH149, respectively (Table 1, Figure S4). Altogether, the type of the fused heterocycle at the phosphaphenalene core appears to influence the bioactivity of the drug; pyrrole leads to improved cytotoxic activity. However, further increasing the bulkiness of the phosphaphenalene with an electron-accepting phenylsulfonyl group does not further enhance the agent's bioactivity.

Based on the remarkable results obtained with system **2**, we further investigated its antiproliferative effects on a series of different cancer cell lines. To this end, in addition to the three glioblastoma cell lines described above, we employed compound **2** on 11 other cancer cell lines including brain metastasis (NCH517, NCH604a and NCH466), meningioma (NCH93 and BenMen-1), IDH-mutant glioma (NCH511b, NCH1618 and NCH3763) and head and neck cancer cell lines (HNO210, HNO199 and HNO97; Table 1, Figures S5–S8). Overall, compound **2** showed antiproliferative effects on all cell lines with mean $IC_{50}$ values around 1.5 μM, even in highly invasive brain metastatic cancer cells. Exceptions were found for NCH89, NCH3763 and HNO97 cell lines with $IC_{50}$ values of 4.00, 5.21 and 5.51 μM, respectively and for IDH-mutant glioma cell line NCH1681 with impressively low $IC_{50}$ values of 0.88 μM.

Motivated by these results, we analyzed the capacity of **2** to induce apoptosis in cancer cell lines derived from brain metastases, meningiomas, IDH-mutant gliomas and head and neck cancers. For this purpose, cells were incubated with different concentrations of **2** for 48 h and subsequently analyzed by flow cytometry (see representative example in Figure 3A). Annexin V and propidium iodide (PI) were used as indicators for apoptosis/necrosis. As expected, compound **2** was able to induce apoptosis/necrosis in all analyzed cell lines. Figure 3A shows the evolution of the cell populations from alive to apoptotic and finally necrotic when increasing the concentration from 0 to 5 μM.

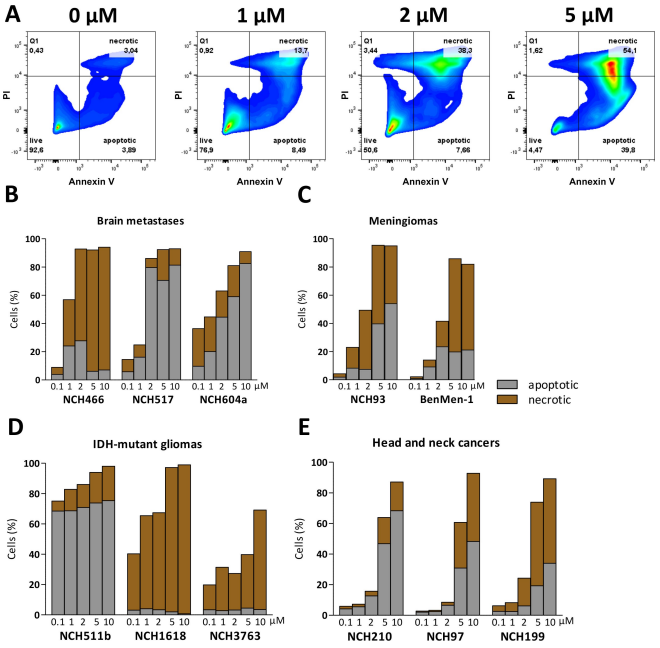


**Figure 3.** Concentration-dependent induction of apoptosis and necrosis. A) Flow cytometry analysis of NCH93 cells without treatment and upon exposure to 1, 2, and 5 μM of compound **2** for 48 h. Stack charts summarize the percentage of apoptotic and necrotic cells of B) brain metastasis, C) meningioma, D) IDH-mutant glioma, and E) head and neck cancer cell lines.

In line with the obtained $IC_{50}$ values (Table 1), brain metastasis and meningioma cell lines appeared to be more sensitive than head and neck cancer cell lines. A drug concentration of 2 μM induced apoptosis/necrosis in more than 50% of cells among NCH466, NCH517, NCH604a and NCH93 (Figure 3B and 3 C). On the contrary, a drug concentration of 5 μM was needed to cause apoptosis/necrosis in more than 50% of cells in head and neck cancer cell lines (Figure 3E).

In line with their improved bioactivity, we further evaluated the spectroscopic properties of compounds **2** and **4** in comparison to a reference compound **C**; that is, the analog structure to **1** but with a pentavalent, oxidized phosphorus atom[21] instead of being attached to the gold atom (Scheme 1, Table 2). In dichloromethane (DCM) solutions, replacing the oxygen at the phosphorus atom from **C** with a sugar-gold moiety (compound **2**) leads to a slight red shift of the absorption maxima from 367 to 372 nm, respectively, and a blue shift of the emission maxima from 450 to 443 nm. In turn, replacing the methyl substituent at the pyrrole moiety in system **2** with a phenylsulfonyl fragment to yield derivative **4**, leads to a relatively blue-shifted absorption maximum at 361 nm and a red-shifted emission maximum at 460 nm (Figure S9a). In contrast to compound **C**, which exhibits a fluorescence quantum yield ($\Phi$) of 80%, both molecules **2** and **4** show $\Phi <$ 1%. As reported earlier,[22] this is attributed to the heavy atom effect from the gold atom.

Overall, complexes **2** and **4** present a positive solvatochromism. In DMSO:water (1:9, *v/v*), the absorption and emission maxima are significantly redshifted comparing to those from

**Table 2.** Selected spectroscopic data of compounds **2**, **4** and **C**.

| Compd. | $\lambda_{max\,abs}$ [nm] | log $\varepsilon$ [L mol$^{-1}$cm$^{-1}$][a] | $\lambda_{max\,em}$ [nm] | $\Delta\nu$ [cm$^{-1}$][b] | $\tau$1; $\tau$2; $\tau$3 [ns][c,d] | $\Phi$ [%][e] |
|---|---|---|---|---|---|---|
| **C**[f] | 367 | 3.90 | 450 | 5026 | 9.9 | 80 |
| **C**[g] | 370 | 3.77 | 470 | 5750 | 18.8 | 63 |
| **2**[f] | 372 | 3.59 | 443 | 4308 | 2.3 | $<1$ |
| **2**[g] | 379 | 3.84 | 462 | 4740 | 0.6(19); 5.6(62); 0.2(19) | 6 |
| **4**[f] | 361 | 3.79 | 460 | 5962 | 1.6(32); 7.1(68) | $<1$ |
| **4**[g] | 366 | 3.90 | 467, 508 (sh) | 5909 | 3.1(24); 13.7(57); 0.1(18.6) | $<1$ |

[a] Molar extinction coefficient. [b] Stokes shift. [c] Fluorescence lifetimes. [d] Numbers in brackets are the relative amplitudes. [e] Fluorescence quantum yields. [f] Physicochemical parameters recorded from $CH_2Cl_2$ solutions. [g] Physicochemical parameters recorded from DMSO/water = 1:9 (*v*/*v*) solutions.

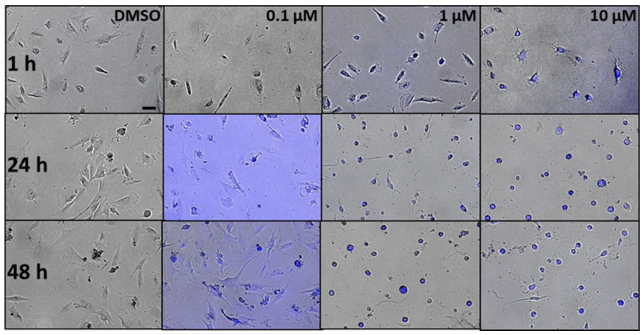


**Figure 4.** Fluorescence microscopy images of glioblastoma cells taken 1, 24 and 48 h after treatment with compound **2** at concentrations of 0, 0.1, 1 and 10 µM. Glioblastoma cells internalize compound **2** after 1 h of treatment at drug concentrations of 1 and 10 µM. Scale bar: 200 µm.

DCM solutions. The absorption spectra of **2** and **4** maximize at 379 and 366 nm, respectively, whereas their emission maxima appear at 462 and 467 nm (Figure S9b). The quantum yield of **4** did not improve in aqueous solutions ($\Phi < 1\%$). However, fortunately, **2** exhibited a significant quantum yield of 6%, which converts it into a potential candidate for future mechanistic studies *in vivo*. Nevertheless, this is still in sharp contrast to the reference oxide **C**, which lacks of heavy atom effect and presents a quantum yield of 63% in DMSO:water (1:9, *v*/*v*) solutions. Importantly, both compounds proved to be stable for weeks under controlled thermodynamic conditions upon repetitive cycles of illumination (Figures S10–S11).

Motivated by the bioactivity and the spectroscopic properties of compound **2**, we investigated the drug uptake kinetics in NCH82 cell line (see the Supporting Information for details). To this end, cells were treated with increasing concentrations of derivative **2** and its drug uptake was monitored with a fluorescence microscope ($\lambda_{ex} = 350$ nm, $\lambda_{em} = 455$ nm; Figure 4). Surprisingly, after only 1 hour of treatment with 10 µM of compound **2**; that is, above the $IC_{50}$ value, cells were able to internalize the compound and started to shrink and detach. Cells treated with 1 µM of derivative **2** started to absorb the compound after 1 h but their death could be observed only after 24 h. When used at a concentration of 0.1 µM, compound **2** started to be internalized after 24 h but cell death was first observed 48 hours after treatment initiation (Figure 4).

All in all, this proof-of-principle experiment demonstrates that the phosphaphenalene–gold(I) complexes are absorbed by the cells within a relatively short period of time. This characteristic, together with their notable spectroscopic properties in aqueous media, converts them into potential candidates to carry out further, future mechanistic investigations on the mode of action. Detailed investigations to this end are currently underway in our laboratories and will be published on their own in the near future.

## Conclusion

Herein, we have demonstrated that the bioactivity of phosphaphenalene gold complexes can be improved by subtle chemical modification of their structural features. Their unique properties allow the electronic distribution over the π-extended core, the bulkiness of the molecules and their photophysical properties to be adjusted. In particular, pyrrole-fused phosphaphenalene derivatives lead to better performances than thiophene-based analogs; it is worth noting that they are stable for weeks. In turn, increasing the bulkiness of the phosphaphenalene moiety while withdrawing electronic density with a phenylsulfonyl fragment not only quenches the fluorescence in both aqueous and organic media but also slightly reduces the antiproliferative activity. On the other hand, sugar derivatives attached to the gold atom provide higher bioactivity than chloride atoms. All in all, pyrrole-fused phosphaphenalene gold complexes possess a remarkable antiproliferative capacity. They inhibit the proliferation of 14 different tumor cell lines derived from glioblastomas, brain metastases, meningiomas, IDH-mutant gliomas and head and neck cancers. Overall, their $IC_{50}$ values are around 1.5 µM; the lowest values are in the sub-micromolar order: 0.73, 0.87 and 0.88 µM for NCH82, NCH149 and NCH1681 cell lines, respectively. In addition, pyrrole-based phosphaphenalene gold complexes appear to sensitize brain metastasis, meningioma, IDH-mutant glioma and head and neck cancer cell lines to apoptosis; they thus reveal a broad applicability. Finally, in proof-of-principle experiments, the spectroscopic properties of the phosphaphenalenes were shown to be suitable for monitoring the cell uptake of drugs. In brief, the broad applicability of the pyrrole-fused phosphaphenalene gold complexes in combination with their notable spectroscopic properties are anticipated to provide new research pathways for a better understanding of these lethal diseases. *In vivo* experiments are currently underway in our laboratories; the results will be published in due time.

## Experimental Section

Deposition Number 2093641 contains the supplementary crystallographic data for this paper. These data are provided free of charge by the joint Cambridge Crystallographic Data Centre and Fachinformationszentrum Karlsruhe Access Structures service.

## *Acknowledgements*

The Organisch-Chemisches Institut of the University of Heidelberg and the UCLM are acknowledged for the support. C. H. M and C. R. N thank the Excellence Initiative (Innovation Fund FRONTIER) of the University of Heidelberg for a grant. Funding from RO4899/4-1 and SBPLY/17/180501/000518 are gratefully acknowledged as well as project RTI2018-101865-A–I00 funded by MCIN/AEI/10.13039/501100011033/ and by FEDER "A way to make Europe". Open Access funding enabled and organized by Projekt DEAL.

## Conflict of Interest

The authors declare no conflict of interest.

## Data Availability Statement

The data that support the findings of this study are available on request from the corresponding author. The data are not publicly available due to privacy or ethical restrictions.

**Keywords:** brain cancer · glioblastoma multiforme · gold complexes · phosphorus heterocycles · phosphaphenalenes · photoluminescence

[1] C. Weiss, in *Ethical Challenges in Cancer Diagnosis and Therapy* (Eds.: A. W. Bauer, R.-D. Hofheinz, J. S. Utikal), Springer International, Cham, **2021**, pp. 15–29.
[2] D. N. Louis, H. Ohgaki, O. D. Wiestler, W. K. Cavenee, P. C. Burger, A. Jouvet, B. W. Scheithauer, P. Kleihues, *Acta Neuropathol.* **2007**, *114*, 97–109.
[3] Q. T. Ostrom, N. Patil, G. Cioffi, K. Waite, C. Kruchko, J. S. Barnholtz-Sloan, *Neurooncology* **2020**, *22*, iv1–iv96.
[4] Q. T. Ostrom, H. Gittleman, P. Farah, A. Ondracek, Y. Chen, Y. Wolinsky, N. E. Stroup, C. Kruchko, J. S. Barnholtz-Sloan, *Neurooncology* **2013**, *15*, ii1–ii56.
[5] R. Stupp, W. P. Mason, M. J. van den Bent, M. Weller, B. Fisher, M. J. B. Taphoorn, K. Belanger, A. A. Brandes, C. Marosi, U. Bogdahn, J. Curschmann, R. C. Janzer, S. K. Ludwin, T. Gorlia, A. Allgeier, D. Lacombe, J. G. Cairncross, E. Eisenhauer, R. O. Mirimanoff, *N. Engl. J. Med.* **2005**, *352*, 987–996.
[6] M. Weller, T. Cloughesy, J. R. Perry, W. Wick, *Neurooncology* **2013**, *15*, 4–27.
[7] M. Esteller, J. Garcia-Foncillas, E. Andion, S. N. Goodman, O. F. Hidalgo, V. Vanaclocha, S. B. Baylin, J. G. Herman, *N. Engl. J. Med.* **2000**, *343*, 1350–1354.
[8] M. E. Hegi, A.-C. Diserens, T. Gorlia, M.-F. Hamou, N. de Tribolet, M. Weller, J. M. Kros, J. A. Hainfellner, W. Mason, L. Mariani, J. E. C. Bromberg, P. Hau, R. O. Mirimanoff, J. G. Cairncross, R. C. Janzer, R. Stupp, *N. Engl. J. Med.* **2005**, *352*, 997–1003.
[9] C. W. Brennan, R. G. W. Verhaak, A. McKenna, B. Campos, H. Noushmehr, S. R. Salama, S. Zheng, D. Chakravarty, J. Z. Sanborn, S. H. Berman, *Cell* **2013**, *155*, 462–477.
[10] S. Roesch, V. Fermi, F. Rominger, C. Herold-Mende, C. Romero-Nieto, *Chem. Commun.* **2020**, *56*, 14593–14596.
[11] P. Hindenberg, C. Romero-Nieto, *Synlett* **2016**, *27*, 2293–2300.
[12] N. Mezailles, P. Floch, *Curr. Org. Chem.* **2006**, *10*, 3–25.
[13] C. Müller, D. Vogt, *Dalton Trans.* **2007**, 5505–5523.
[14] P. L. Floch, in *Phosphorous Heterocycles I* (Ed.: R. K. Bansal), Springer, Berlin, **2008**, pp. 147–184.
[15] T. Baumgartner, *Acc. Chem. Res.* **2014**, *47*, 1613–1622.
[16] M. Stolar, T. Baumgartner, *Chem. Asian J.* **2014**, *9*, 1212–1225.
[17] D. Joly, P.-A. Bouit, M. Hissler, *J. Mater. Chem. C* **2016**, *4*, 3686–3698.
[18] E. Regulska, C. Romero-Nieto, *Dalton Trans.* **2018**, *47*, 10344–10359.
[19] E. Regulska, P. Hindenberg, C. Romero-Nieto, *Eur. J. Inorg. Chem.* **2019**, *2019*, 1519–1528.
[20] E. Regulska, C. Romero-Nieto in *Photochemistry, Volume 48*, Royal Society of Chemistry, **2020**, pp. 376–410.
[21] C. Romero-Nieto, A. López-Andarias, C. Egler-Lucas, F. Gebert, J.-P. Neus, O. Pilgram, *Angew. Chem. Int. Ed.* **2015**, *54*, 15872–15875; *Angew. Chem.* **2015**, *127*, 16098–16102.
[22] P. Hindenberg, A. López-Andarias, F. Rominger, A. de Cózar, C. Romero-Nieto, *Chem. Eur. J.* **2017**, *23*, 13919–13928.
[23] P. Hindenberg, J. Zimmermann, G. Hernandez-Sosa, C. Romero-Nieto, *Dalton Trans.* **2019**, *48*, 7503–7508.
[24] E. Regulska, S. Christ, J. Zimmermann, F. Rominger, G. Hernandez-Sosa, C. Romero-Nieto, *Dalton Trans.* **2019**, *48*, 12803–12807.
[25] E. Yue, L. Dettling, J. A. W. Sklorz, S. Kaiser, M. Weber, C. Müller, *Chem. Commun.* **2022**, *58*, 310–313.
[26] M. Deponte, S. Urig, L. D. Arscott, K. Fritz-Wolf, R. Réau, C. Herold-Mende, S. Koncarevic, M. Meyer, E. Davioud-Charvet, D. P. Ballou, C. H. Williams, K. Becker, *J. Biol. Chem.* **2005**, *280*, 20628–20637.
[27] E. Jortzik, M. Farhadi, R. Ahmadi, K. Tóth, J. Lohr, B. M. Helmke, S. Kehr, A. Unterberg, I. Ott, R. Gust, V. Deborde, E. Davioud-Charvet, R. Réau, K. Becker, C. Herold-Mende, *Biochim. Biophys. Acta Proteins Proteomics* **2014**, *1844*, 1415–1426.
[28] S. S. Gunatilleke, A. M. Barrios, *J. Med. Chem.* **2006**, *49*, 3933–3937.
[29] S. Kenzler, M. Kotsch, A. Schnepf, *Eur. J. Inorg. Chem.* **2018**, *2018*, 3840–3848.
[30] E. Viry, E. Battaglia, V. Deborde, T. Muller, R. Reau, E. Davioud-Charvet, D. Bagrel, *ChemMedChem* **2008**, *3*, 1667–1670.
[31] M. Deponte, S. Urig, L. D. Arscott, K. Fritz-Wolf, R. Reau, C. Herold-Mende, S. Koncarevic, M. Meyer, E. Davioud-Charvet, D. P. Ballou, C. H. Williams Jr., K. Becker, *J. Biol. Chem.* **2005**, *280*, 20628–20637.

Manuscript received: December 23, 2021
Accepted manuscript online: March 16, 2022
Version of record online: April 19, 2022